Energy 111 (2016) 923–932

Contents lists available at ScienceDirect

Energy

journal homepage: www.elsevier.com/locate/energy

Parametric optimization and exergetic analysis comparison of subcritical and supercritical organic Rankine cycle (ORC) for biogas fuelled combined heat and power (CHP) engine exhaust gas waste heat

Hüseyin Yağlı [a], Yıldız Koç [a], Ali Koç [a, *], Adnan Görgülü [b], Ahmet Tandiroğlu [c]

[a] Iskenderun Technical University, Hatay, Turkey
[b] Siemens AG, Duisburg, Germany
[c] Erzincan University, Erzincan, Turkey

ARTICLE INFO

Article history:
Received 1 January 2016
Received in revised form
30 April 2016
Accepted 28 May 2016
Available online 17 June 2016

Keywords:
Combined heat and power (CHP)
Organic rankine cycle (ORC)
Parametric optimization
Subcritical
Supercritical
Exhaust gas
Exergy

ABSTRACT

In this paper, a subcritical and supercritical organic Rankine cycle (ORC) are designed to recover exhaust gas waste heat of biogas fuelled combined heat and power (CHP) engine. The CHP engine is located in Belgium and uses biogas as fuel which is produced from the digestion of domestic wastes by anaerobic digestion. R245fa is selected as working fluid. First, the system parameters as net power, mass flow rate, pumps total power consumption, total evaporator exergy inlet, thermal efficiency and exergy efficiency are improved by changing turbine inlet temperature and pressure. After which second low analysis of the overall system and system components are determined for the best performed subcritical and supercritical cycles. Compared with subcritical ORC, the supercritical ORC has shown better performance. The best performed cycle net power, thermal efficiency and exergy efficiency are evaluated as 79.23 KW, 15.51% and 27.20% for subcritical ORC and 81.52 kW, 15.93% and 27.76% for supercritical ORC, respectively.
© 2016 Elsevier Ltd. All rights reserved.

1. Introduction

Despite the accelerated growth of renewable energy systems, more than three-quarter of world's energy need is supplied from fossil fuels [1]. The increasing consumption of the fossil fuels leads to realizing that global warming and rapid changes in climate needs to be reduced by developing green power systems [2–4]. The utilization rate of renewable sources is 20% these days and this level is planned to be increased by 50% to a level of 30% over the next two years [1]. Renewable energy sources include biomass [5], geothermal [6], solar [7] and the wind [8,9]. Biogas is also one of the most important renewable energy fuels which is produced by anaerobic digestion of organic based wastes [10]. Combined heat and power (CHP) is used mostly to converting biogas energy [11]. The maximum efficiencies up to 46% of the CHP engines have been reported and the big amount of biogas energy is rejected to the environment as waste heat in several forms [12]. Abusoglu and Kanoglu 2009, presented the exergetic and thermodynamic analyses of a cogeneration system which is powered by a diesel engine. The paper focused on exergy destructions, efficiencies and exergetic cost distributions for plants and components. Further examination of the results showed that recovering the waste heat of exhaust gas improved cycle performance positively [13]. He at al. 2011, studied on waste heat recovery of internal combustion engine. The paper presented a steady state experiment, energy and exergy analysis of exhaust gas. The energy flow of the engine stated that almost two third of the heat of the combusted fuel is released to the environment as waste, mostly as exhaust gas and the rest is released in the cooling process [14].

Organic Rankine cycle could be used to improve the efficiency of the CHP engine by recovering waste heat. Compared to conventional Rankine cycle, the organic Rankine cycle (ORC) has many

* Corresponding author. Faculty of Mechanics, Department of Mechanical Engineering, Iskenderun Technical University, 31200, Iskenderun, Hatay, Turkey.
E-mail addresses: hsyn.yagli@gmail.com (H. Yağlı), yildizkoc66@hotmail.com (Y. Koç), alikoc59@hotmail.com (A. Koç), adnan.goerguelue@gmail.com (A. Görgülü), atandiroglu@erzincan.edu.tr (A. Tandiroğlu).

http://dx.doi.org/10.1016/j.energy.2016.05.119
0360-5442/© 2016 Elsevier Ltd. All rights reserved.

advantages to recovering waste heat. Thermal efficiency and net power production of the organic Rankine cycle is higher than steam Rankine cycle for low temperature waste heat sources because working fluids of the ORC are organic based and have lower boiling temperature [12,15]. There have been many studies that have attempted to explain designing, working fluid selection and optimizing of the ORC. Yamamoto et al., 2001, studied the cycle performance of the ORC basis both experimentally and theoretically. Results show that the cycle with HCFC-123 gave more turbine power and improves the performance of cycle [16]. Hettiarachchi et al., 2007, presented optimum design criteria for the ORC which utilized the low temperature geothermal heat source. The ratio of the total heat exchanger surfaces for net power production was used as target function [17]. Chen et al., 2012, described a new design method for ORC with benzene as working fluid and sample conditions were defined to investigate optimum working parameters [18]. The performance of the different working fluids for low temperature heat sources was conducted by Lakew and Bolland 2010, they found that R227ea had the best performance for source temperature in the range of 80–160 °C and R245fa was the most efficient working fluid between 160 °C and 200 °C [19]. Tian et al., 2014, described working fluid selection for a high-temperature regenerative transcritical dual-loop ORC. Results showed that toluene had highest net power, energy conversion efficiency and exergetic efficiency [20]. The thermoeconomic optimization of three trigeneration systems was conducted by Al-Sulaiman et al., 2013, they found that the furthest exergy efficiency was nearly 38% for the SOFC-trigeneration system, 28% for the biomass trigeneration system and 18% for the solar trigeneration system [21].

For the subcritical and supercritical ORC, many studies have been performed. Gu and Sato 2001 found the maximum thermal efficiency of a geothermal-sourced supercritical ORC by considering suitable working fluid and optimization of the system state parameters [22]. Schuster et al., 2010 analysed the optimization of the thermal efficiency of a supercritical organic Rankine cycle by taking into account different working fluids [23]. Algieri and Morrone 2012, described the energetic performance of a high temperature subcritical and transcritical ORC for a biomass power plant. The operating conditions and regeneration effects on cycle performance was conducted [24]. Furthermore, many studies investigated waste heat recovery of internal combustion engines. Srinivasan et al., 2010, analysed recoverable energy potential of a dual fuel low temperature combustion engine driving an ORC. Fuel conversion efficiency of the engine increased around 7% while NO_x and CO_2 emissions decreased 18% [25]. Qiu et al., 2012, investigated experimentally a biomass heat sourced ORC based micro-CHP. The analysis results for 50 kW_{th} micro-CHP shows that 861 W electricity production and 47.26 kW_{th} heat is possible. Meanwhile, electricity generation efficiency and CHP efficiency were calculated to be 1.41% and 78.69%, respectively [26]. Tian et al., 2012, optimized fluids and parameters of the ORC used to recover exhaust waste heat of an internal combustion engine [12]. Kölsch and Radulovic 2015 studied on the usability of diesel engine waste heat by organic Rankine cycle. Toluene, solkatherm and methanol are used as a working fluid of cycle [27].

From the papers above, it is obvious that only several papers have examined the internal combustion engine waste heat which was generally diesel fuelled engines. Furthermore, there are very few studies a combination of both subcritical and supercritical ORC in which just a few of studies have compared their parametric optimization results. In addition, only limited studies involve optimization of the cycle state parameter, exergetic analysis of the system and destruction in the cycle components for both subcritical and supercritical together. This study has playing an important role on ORC systematic. The effects of turbine inlet temperatures and pressures on ORC system parameters are demonstrated for exhaust gas waste heat of the biogas fuelled CHP engine. Additionally, the critical point is coming from on this study that the biogas fuelled CHP engine has used with subcritical and supercritical conditions together; as one of the limited work in literature.

The present work aims to investigate the parametric study, optimization and performance comparison of subcritical and supercritical organic Rankine cycle for the exhaust gas of the two biogas fuelled CHP engine, which is located in Belgium. Influence of turbine inlet temperature and turbine inlet pressure on performance parameters as net power production, mass flow rate, pumps total power consumption, total exergy inlet rate of the evaporator, thermal efficiency and exergetic efficiency are analysed and performance comparison of the subcritical and supercritical ORC is evaluated. After the performance improvement of cycles produced by changing the turbine inlet pressure and temperature for the subcritical and supercritical ORC, the energy and exergy analysis of the best performed cycles are made using balance equations.

2. System description

2.1. Biogas power plant

The schematic view of the biogas power plant is shown in Fig. 1. This plant in Belgium has two internal combustion engines. The total installed electricity capacity of biogas power plant is 1611 kW and excess heat of the jacket water (JW) is used in the heating of the houses located around the power plant. The power production plant consists of two successive processes while the first is biogas production and purification part, the second part is power production part which includes an internal combustion engine and local house heating loop coupled with the JW.

The domestic waste in Belgium is being collected to use as a source for biogas fermentation. Biogas production for power engine includes the various preparation steps. First of all, domestic waste of houses is purified from non-organic wastes (e.g., plastics, can and glass) and then organic wastes are charged to the digestion well. After the starting of the anaerobic fermentation, the produced biogas will be collected for purification. In the second step, the biogas passes through the desulphurizer and dehumidifier sections, after which the chemical compounds of the purified biogas includes 55% of CH_4 and 45% of CO_2. In the last step, the purified biogas is stored in the tank before mixing with air.

2.2. Combined heat and power (CHP) engine

In the present paper, the exhaust gas of a twelve-cylinder turbocharged biogas engine is investigated as a topping system.

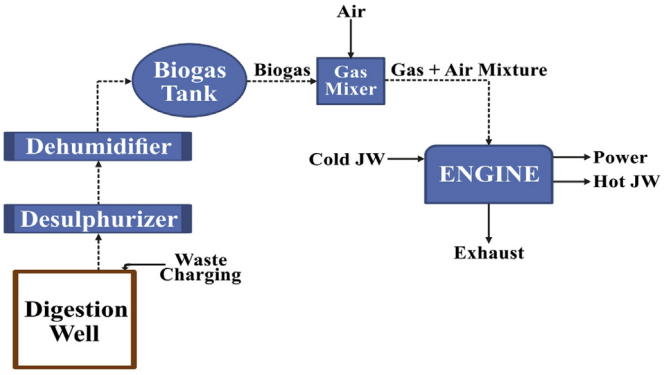


Fig. 1. Schematic view of the biogas power plant.

The engine produces 534 kW of electricity while the excess heat of the jacket water used for domestic home heating. This plant has two CHP engines which are shown in Fig. 2 schematically. As shown in the figure, the biogas (green line) mixes with air (sky blue line) and then goes through the compressor which is powered by exhaust driving the turbine. After that the mixture is heated up in the heat exchanger by jacket water (red line). The lubrication oil (blue line) of the engine is supplied from feed unit throughout the time that motor keeps running. The exhaust gas of the engine (brown line) goes through the turbine then discharges to the atmosphere at a temperature range 450–485 °C. Before cooling the jacket water in air cooler, it passes through a heat exchanger to heat home heating loop (pink line) between 87 and 91 °C.

To have better results, the CHP engine is assumed to be operated at nominal conditions which are stated in Table 1.

The exhaust gas temperature is changing during the year which depends on season and environment temperature. The exhaust gas temperature fluctuates between 450 °C and 500 °C. The design temperature of the gas for organic Rankine cycle is assumed as 450 °C to get mean power production capacity. The total exhaust gas mass flow rate of engines is measured as 1.63 kg/s.

2.3. Organic Rankine cycle

The organic Rankine cycle (ORC) has an almost identical working principle to conventional Rankine cycle but different working fluid and heat source range. The ORC uses organic based working fluids and low temperature heat sources above 80 °C while conventional Rankine cycle uses steam as working fluid and high temperature heat sources above 500 °C. The general schematic view of the ORC coupled CHP engine is shown in Fig. 3. The CHP engine releases excess heat of the system in two ways which are jacket cooling water and exhaust gas. The jacket cooling water is used for domestic heating, and the exhaust gas discharges to the atmosphere. An ORC is designed and optimized parametrically to recover the excess heat which is wasted in the current system.

The designed ORC has four main components which are hot side components (preheater, evaporator, and superheater), expansion component (turbine), cooling side component (condenser) and compression component (pump). The hot side of the ORC is designed with three different components to capture the excess heat of the gas easily and to evaluate superheated vapor at the inlet of the turbine.

Table 1
Nominal operating conditions of each CHP engine.

Parameter	Value	Unit
Number of engines	2	–
Mechanical efficiency	40.6%	–
Electrical efficiency	39.3%	–
Thermal efficiency (exhaust cooled to 180 °C)	37.2%	–
Engine electrical power	534	kW_e
Exhaust temperature	450	°C
Exhaust mass flow rate (wet)	2981	kg/h
Exhaust power (cooled to 180 °C)	285	kW

In the study, the ORC is designed for subcritical and supercritical conditions. The temperature and entropy change diagram for the subcritical and supercritical cycles are given in Fig. 4.

In the case of the subcritical cycle, the turbine inlet pressure is below critical pressure when compared to the supercritical cycle. In both the subcritical and supercritical cycles, turbine efficiency, pump efficiency, general electrical efficiency, cooling water inlet temperature and condensation pressure are assumed as constant during designing and optimizing process given in Table 2. The pressure drops in pipes, condenser and evaporator are ignored when the thermodynamic properties are estimated but the pressure drop in preheater and superheater are assumed as 0.05 bar.

3. Mathematic model and working fluid

3.1. Energy and exergy analysis

A detailed analysis of the subcritical and supercritical ORC is essential while deciding upon the optimal cycle condition to

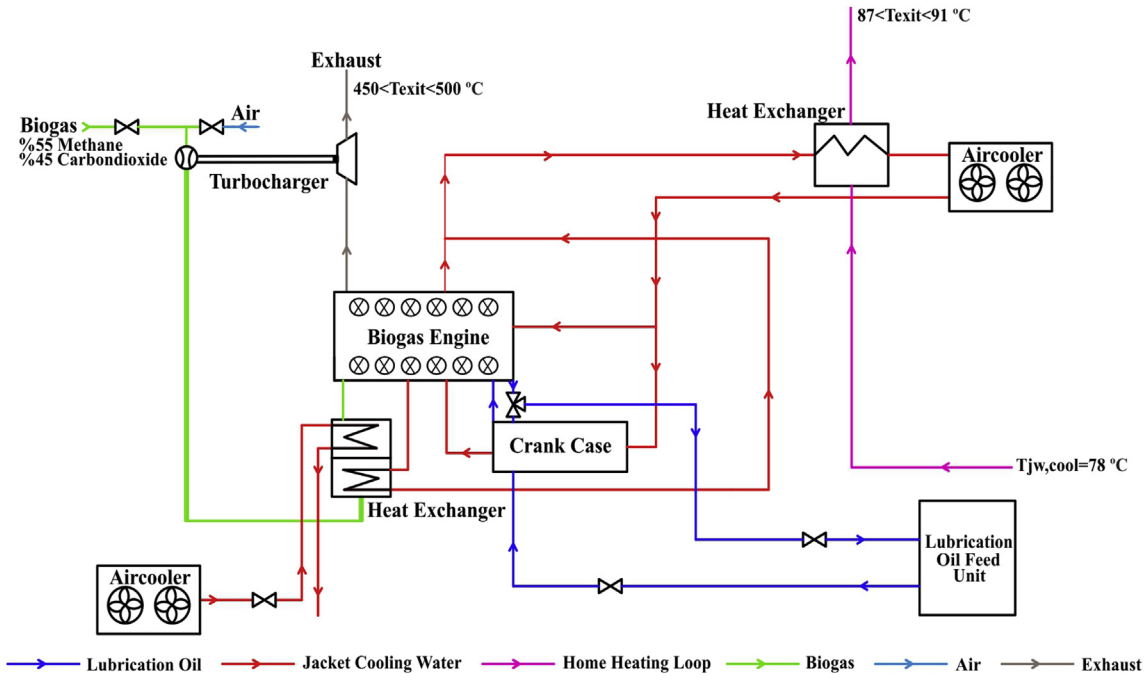


Fig. 2. The schematic of the CHP engine.

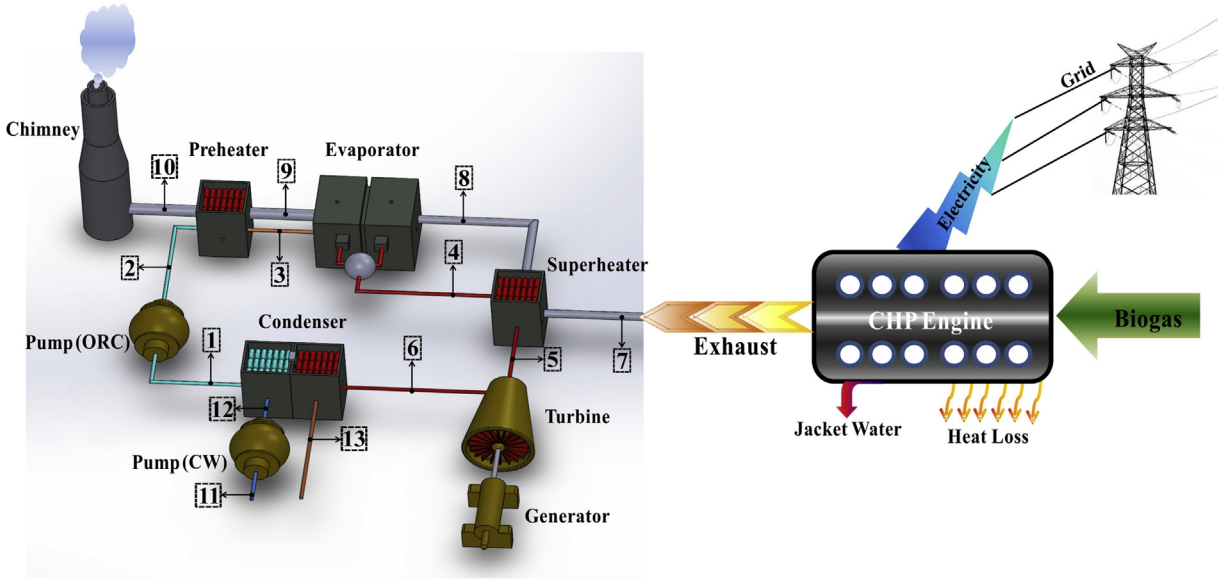


Fig. 3. The schematic of the ORC coupled CHP engine.

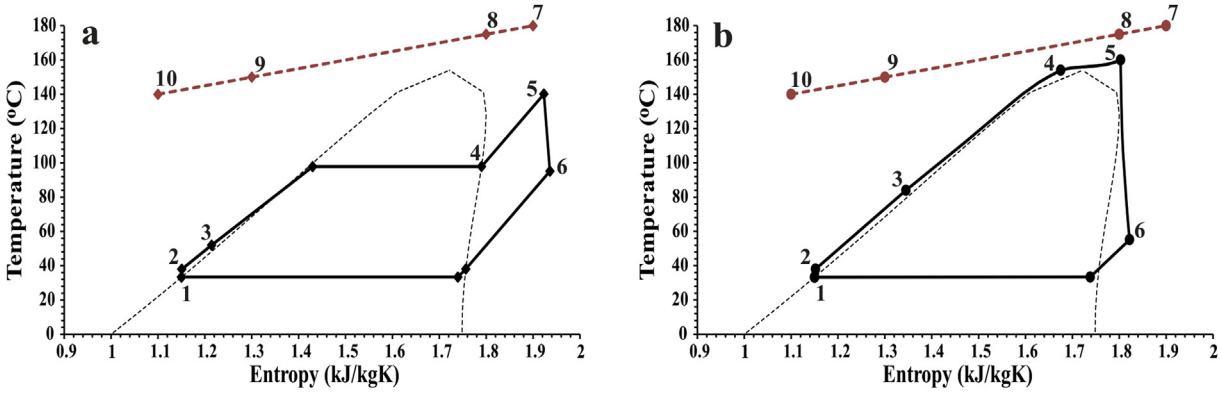


Fig. 4. Temperature and entropy change diagram for the (a) subcritical and (b) supercritical ORC.

perform. This paper does not only include energy-based analysis of the systems but also it includes exergy-based analysis of the cycles. Because only energy analysis of the system is not enough to have an ultimate decision on the system performance without exergy analysis. The mass, energy and exergy analysis of the ORC is made by using common balance formulation which can be written as:

$$\sum \dot{m}_{in} = \sum \dot{m}_{out} \tag{1}$$

$$\dot{Q} + \dot{W} = \sum (\dot{m}h)_{out} - \sum (\dot{m}h)_{in} \tag{2}$$

Table 2
ORC design and parametric optimization assumptions.

Parameter	Value	Unit
Turbine efficiency	88%	–
Pump efficiency	80%	–
Generator electrical efficiency	88.5%	
Condenser cooling water inlet temperature	25.008	°C
Condensation pressure	2	bar

$$\dot{E}_{ex;in} = \dot{E}_{ex;out} + \dot{E}_{ex;dest} \tag{3}$$

where $\dot{E}_{ex;in}$, $\dot{E}_{ex;out}$ and $\dot{E}_{ex;dest}$ refers to exergy flow inlet, exergy flow outlet and exergy destruction, respectively. $\dot{E}_{ex}$ refers to exergy flow and calculated by:

$$\dot{E}_{ex} = \dot{m}\psi \tag{4}$$

$\psi$is specific exergy flow is found by:

$$\psi = (h - h_0) - T_0(s - s_0) \tag{5}$$

Work has a 100% exergy efficiency, but the heat has an exergy efficiency of less than 100%. Therefore, in order to determine the exergy flow of heat ($\dot{E}_{ex;H}$), the following equation should be used:

$$\dot{E}_{ex;H} = \left(1 - \frac{T_0}{T_{HS}}\right)\dot{Q} \tag{6}$$

where T_0 is the room temperature or death state temperature (18 °C), and T_{HS} is the temperature of heat transfer surface which taken as average value of the inlet and outlet temperature of the working fluid in component.

Exergy calculations of each component were made using the exergy balance equation; then, the exergy efficiencies were calculated using the equations given in Table 3.

The overall cycle energy and exergy efficiency are described by:

$$\eta_{ORC} = \frac{\dot{W}_{net}}{\dot{Q}_{in}} \tag{7}$$

$$\varepsilon_{ORC} = \frac{\dot{E}_{ex;out}}{\dot{E}_{ex;in}} = \frac{\dot{W}_{net}}{\dot{E}_{ex;in}} \tag{8}$$

All determinations were made by assuming steady state conditions, negligible kinetic and potential energies, and an ambient temperature of 18 °C.

3.2. Working fluid

Working fluid selection of an ORC has great importance while finding out the most feasible ORC to perform for certain conditions. There are many fluid selection criteria like thermodynamic properties (critical temperature, critical pressure, enthalpy of evaporation etc.), types of fluids (wet, dry, isentropic), environmental effect, unit price. When all these criteria are considered, R245fa gives better results for subcritical and supercritical ORC's. The working fluid R245fa has lower critical pressure, critical temperature, enthalpy of evaporation compared with water. As shown in Fig. 5, while R245fa is isentropic, water is a wet type fluid and not comfortable for recovering low heat sources because of its high boiling point.

Because of all these reasons, R245fa is selected as working fluid of both subcritical and supercritical ORC's. R245fa has the critical temperature of 154 °C, the critical pressure of 36.5 bar and the maximum temperature of 166.85 °C above which chemical decomposition and structural deterioration of the R245fa starts [33].

4. Results and discussion

4.1. Subcritical ORC

The subcritical ORC has lower turbine inlet pressure than critical pressure. The designed cycles have the pressure between 4 bar and 30 bar while turbine inlet temperature changes in the range of 56 °C and 166 °C. The minimum temperature of the cycle under the constant pressure is calculated from saturation temperature of the R245fa at turbine pressure. Because of the chemical decomposition and structural deterioration of the working fluid over its maximum temperature, the maximum temperature of the cycle is restricted below the maximum temperature of the working fluid [33]. The effect of the turbine inlet temperature and pressure on the net power, mass flow rate, pumps total power consumption, total evaporator exergy inlet, thermal efficiency and exergy efficiency of subcritical ORC are shown in Fig. 6.

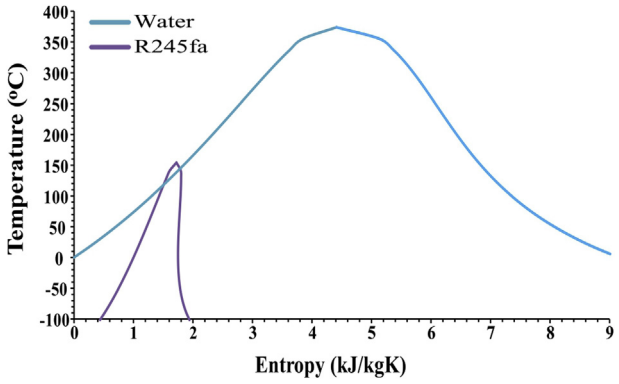


Fig. 5. Saturation curves of R245fa and water [32].

The mass flow rate, pumps total power consumption and total evaporator exergy inlet decrease with increasing temperature at constant pressure (Fig. 6b–d). However, the net power, thermal efficiency and exergy efficiency of subcritical ORC show three different trends with increasing temperature at constant pressure. The first trend is a decrease of the results up to 12 bar of turbine inlet pressure. The second trend of the results is an increase with rising temperature until a certain point and then it starts to decrease up to the maximum temperature between 12 bar and 24 bar of turbine inlet pressure. The last trend is an increase with rising temperature over 24 bar of turbine inlet pressure (Fig. 6a, e, f). The non-linear changes of the net power, thermal efficiency and exergy efficiency of subcritical ORC occur because of some reasons. One of the most important reasons is non-linear changes in enthalpy and mass flow rate. The subcritical ORC has the best performance parameters at 30 bar and 166 °C but this temperature is close to the maximum temperature of the R245fa. Therefore, the optimal subcritical ORC parameter to perform is assumed as 30 bar and 165 °C to maintain cycle performance and prevent the working fluid from chemical decomposition. The net power, thermal efficiency and exergy efficiency of subcritical ORC are determined as 79.23 kW (net power out per mass flow rate=44.04 kj/kg), 15.51% and 27.20% at 30 bar and 165 °C, respectively. Tian et al., 2012 designed a subcritical ORC for exhaust gas waste heat of an internal combustion engine which calculated the net power out per mass flow rate and thermal efficiency as 46 kj/kg and 13% for 30 bar of turbine inlet pressure, respectively [12]. Shengjun et al., 2011 calculated thermal efficiency of a low temperature ORC as nearly 10.65% at 8.7 bar and 84 °C of turbine inlet parameters. In this paper, the thermal efficiency of the subcritical ORC is calculated as

Table 3
Energy and exergy balance model of each component of the ORC [28–31].

Components	Energy balance model	Exergy balance model
Preheater	$\dot{Q}_{ph} = \dot{m}_{ORC}(h_3 - h_2)$	$\dot{E}_{ph,des} = \dot{m}_{exh}(\psi_9 - \psi_{10}) - \dot{m}_{ORC}(\psi_3 - \psi_2)\varepsilon_{ph} = \frac{\dot{m}_{ORC}(\psi_3 - \psi_2)}{\dot{m}_{exh}(\psi_9 - \psi_{10})}$
Evaporator	$\dot{Q}_e = \dot{m}_{ORC}(h_4 - h_3)$	$\dot{E}_{e,des} = \dot{m}_{exh}(\psi_8 - \psi_9) - \dot{m}_{ORC}(\psi_4 - \psi_3)\varepsilon_e = \frac{\dot{m}_{ORC}(\psi_4 - \psi_3)}{\dot{m}_{exh}(\psi_8 - \psi_9)}$
Superheater	$\dot{Q}_{sh} = \dot{m}_{ORC}(h_5 - h_4)$	$\dot{E}_{sh,des} = \dot{m}_{exh}(\psi_7 - \psi_8) - \dot{m}_{ORC}(\psi_5 - \psi_4)\varepsilon_{sh} = \frac{\dot{m}_{ORC}(\psi_5 - \psi_4)}{\dot{m}_{exh}(\psi_7 - \psi_8)}$
Turbine	$\dot{W}_t = \dot{m}_{ORC}(h_5 - h_6)\eta_t = \frac{(h_5 - h_6)}{(h_5 - h_{6s})}$	$\dot{W}_{t,rev} = \dot{m}_{ORC}(\psi_5 - \psi_6)\dot{E}_{t,des} = \dot{W}_{t,rev} - \dot{W}_t\varepsilon_t = \frac{\dot{W}_t}{\dot{W}_{t,rev}}$
Condenser	$\dot{Q}_c = \dot{m}_{ORC}(h_6 - h_1)$	$\dot{E}_{c,des} = \dot{m}_{ORC}(\psi_6 - \psi_1) - \dot{m}_{CW}(\psi_{13} - \psi_{12})\varepsilon_c = \frac{\dot{m}_{CW}(\psi_{13} - \psi_{12})}{\dot{m}_{ORC}(\psi_6 - \psi_1)}$
Pump (ORC)	$\dot{W}_{p,ORC} = \dot{m}_{ORC}(h_2 - h_1)\eta_{p,ORC} = \frac{(h_{2s} - h_1)}{(h_2 - h_1)}$	$\dot{W}_{p,ORC,rev} = \dot{m}_{ORC}(\psi_2 - \psi_1)\dot{E}_{p,ORC,des} = \dot{W}_{p,ORC} - \dot{W}_{p,ORC,rev}\varepsilon_{p,ORC} = \frac{\dot{W}_{p,ORC,rev}}{\dot{W}_{p,ORC}}$
Pump (CW)	$\dot{W}_{p,CW} = \dot{m}_{CW}(h_{12} - h_{11})\eta_{p,CW} = \frac{(h_{12s} - h_{11})}{(h_{12} - h_{11})}$	$\dot{W}_{p,CW,rev} = \dot{m}_{CW}(\psi_{12} - \psi_{11})\dot{E}_{p,CW,des} = \dot{W}_{p,CW} - \dot{W}_{p,CW,rev}\varepsilon_{p,CW} = \frac{\dot{W}_{p,CW,rev}}{\dot{W}_{p,CW}}$

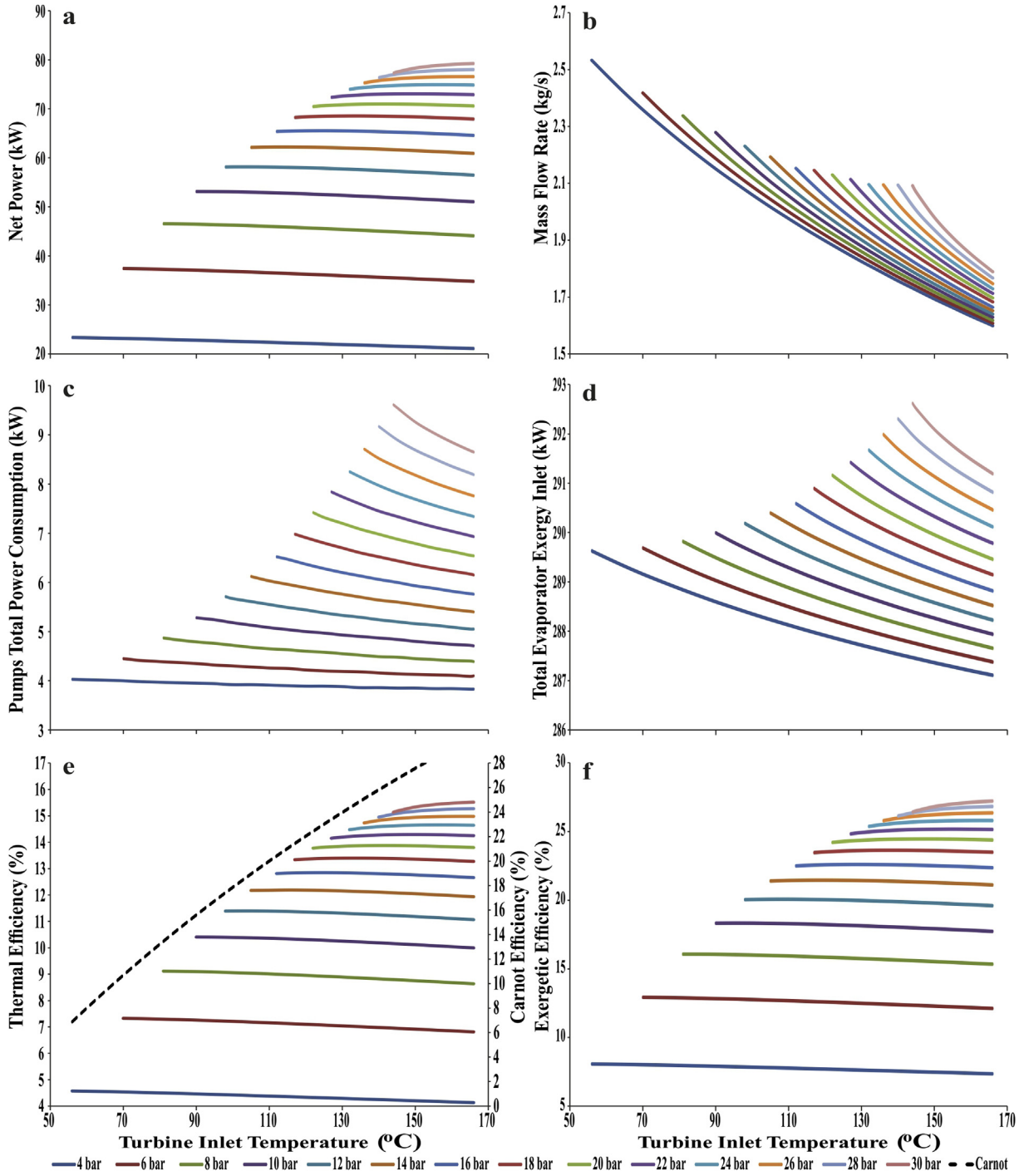


Fig. 6. Effect of turbine inlet temperature and pressure on the (a) net power, (b) mass flow rate, (c) pumps total power consumption, (d) total evaporator exergy inlet, (e) thermal efficiency and (f) exergy efficiency of subcritical ORC.

10.1% at 8.7 bar and 84 °C of turbine inlet parameters [34]. In addition to these papers, Braimakis et al., 2015 determined maximum exergetic efficiency (at 32 bar) with respect to heat source temperature as 28% for a subcritical ORC with R245fa [35]. The present study shows similar maximum exergetic efficiency results as 27.52% for turbine inlet pressure of 32 bar.

4.2. Supercritical ORC

The supercritical ORC has higher turbine inlet pressure than critical pressure. The designed cycles have the pressure between 30 bar and 46 bar while turbine inlet temperature changes between 140 °C and 166 °C. The starting pressure of the cycle is selected below the critical pressure level to show the transition from subcritical to supercritical ORC. The minimum temperature of the cycle under the constant pressure is calculated from saturation temperature of the R245fa at turbine inlet pressure. Because of the chemical decomposition and structural deterioration of the working fluid over its maximum temperature, the maximum temperature of the cycle is restricted below the maximum temperature of

the working fluid [33]. The effect of the turbine inlet temperature and pressure on the net power, mass flow rate, pumps total power consumption, total evaporator exergy inlet, thermal efficiency and exergy efficiency of supercritical ORC are shown in Fig. 7.

The net power, mass flow rate, pumps total power consumption, total evaporator exergy inlet, thermal efficiency and exergy efficiency of supercritical ORC increase with increasing turbine inlet pressure at constant temperature. Moreover, mass flow rate, pumps total power consumption and total evaporator exergy inlet decrease with increasing temperature at constant pressure (Fig. 7b, c, d). The net power, thermal efficiency and exergy efficiency of the cycle increase with increasing temperature. After the 36 bar of turbine inlet pressure, the system starts to work under the supercritical condition where system shows a quick increase of net power, thermal efficiency and exergetic efficiency with rising temperature (Fig. 7a, e, f). The system has better performance with increasing temperature up to the pressure of 38 bar. Above the 38 bar system performance increases with temperature but does not show better performance parameters than the performance of 38 bar. Because the maximum temperature of the supercritical ORC

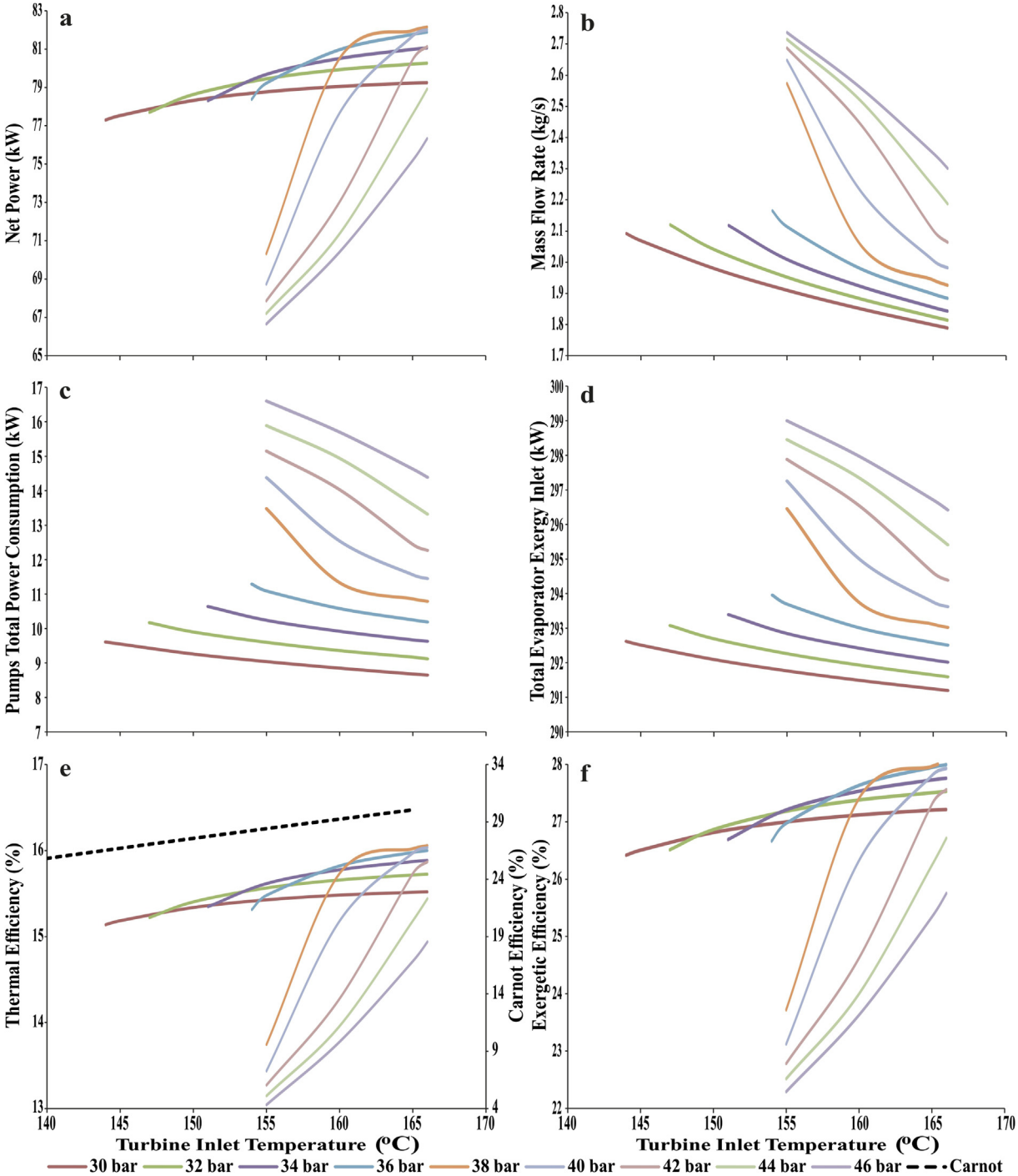


Fig. 7. Effect of turbine inlet temperature and pressure on the (a) net power, (b) mass flow rate, (c) pumps total power consumption, (d) total evaporator exergy inlet, (e) thermal efficiency and (f) exergy efficiency of supercritical ORC.

is limited at 166 °C which is equal to the maximum temperature of the R245fa. Above the maximum temperature, chemical decomposition and structural deterioration of the working fluid starts [33]. As shown in Fig. 8, over the 38 bar of turbine inlet pressure at the beginning time of the expansion, working fluid goes into saturated liquid-vapor mixture zone due to the limitation of maximum working temperature as 166 °C. Therefore, the net power, energy and exergy efficiency of the supercritical ORC over the 38 bar of turbine inlet pressure is not shows better performance than 38 bar of pressure conditions. The supercritical ORC has the best net power, thermal efficiency and exergy efficiency values at 38 bar and 163 °C as 81.52 kW, 15.93% and 27.76%, respectively. Schuster et al., 2010 calculated the thermal efficiency of the supercritical ORC at 37.5 bar and 163 °C as %18 which is similar to our calculations at the same conditions [23]. In spite of chemical decomposition and structural deterioration in the organic fluids above the maximum temperature, the study was analysed the supercritical ORC with R245fa over the maximum temperature of the working fluid (up to 200 °C) [23]. Braimakis et al., 2015 determined variation of the exergetic efficiency with respect to heat source temperature as between almost 17% and 32% for a supercritical ORC with R245fa [35]. The present study shows similar exergetic efficiency results (between 22% and 28%) for turbine inlet temperature from 155 °C to 166 °C.

4.3. Exergetic comparison of the best performed subcritical and supercritical ORC

The best performed subcritical and supercritical ORC evaluated at 30 bar 165 °C and 38 bar and 163 °C, respectively. The evaluated flow parameters of the pipes of improved subcritical and supercritical ORC are given in Table 4. As seen in the table, the pressure drops in pipes, condenser and evaporator are ignored but the pressure drops in preheater and superheater are assumed as 0.05 bar.

The exergy exit and destruction rate of the improved subcritical and supercritical ORC are shown in Fig. 9. The exergy inlet of each component is determined as the sum of the exit and destructed exergy; thus, the sum of each column of the components shown yields the exergy inlet of components in the ORC. The maximum destruction of the exergy which took place in evaporator has a value of 74.51 kW for subcritical and 58.14 kW for supercritical ORC, respectively.

The exergy efficiency of the improved subcritical and supercritical ORC components are given in Fig. 10. The smallest exergy efficiency calculated at preheater. The overall exergy efficiency of the subcritical and supercritical ORC is determined as 27.20% and

Table 4
The evaluated flow parameters of the pipes of improved subcritical and supercritical ORC.

Pipe	P	T	h	$\dot{m}$	ρ	v	s	ψ
	bar	°C	kJ/kg	kg/s	kg/m^3	m^3/kg	kJ/kgK	kJ/kg
30 bar 165 °C (Subcritic)								
1	2.00	33.35	243.59	1.80	1315.55	0.000760	1.15	2.54
2	30.10	34.77	246.25	1.80	1321.23	0.000757	1.15	4.70
3	30.05	79.80	308.82	1.80	1186.09	0.000843	1.34	12.10
4	30.05	143.29	487.90	1.80	232.33	0.004304	1.79	60.05
5	30.00	165.00	530.08	1.80	163.24	0.006126	1.89	73.39
6	2.00	85.63	480.40	1.80	9.33	0.107197	1.91	18.16
7	1.00	450.00	465.44	1.63	0.48	2.075798	7.78	173.49
8	1.00	406.73	418.90	1.63	0.51	1.953540	7.72	146.19
9	1.00	218.29	221.25	1.63	0.71	1.412088	7.38	47.55
10	1.00	150.77	152.19	1.63	0.82	1.219309	7.22	22.41
11	1.00	25.00	104.93	20.43	997.05	0.001003	0.37	0.35
12	2.00	25.01	105.05	20.43	997.09	0.001003	0.37	0.45
13	1.50	30.01	125.91	20.43	995.67	0.001004	0.44	1.06
38 bar 163 °C (Supercritic)								
1	2.00	33.35	243.59	1.98	1315.55	0.000760	1.15	2.54
2	38.10	35.17	247.01	1.98	1322.80	0.000756	1.15	5.31
3	38.05	82.92	313.38	1.98	1180.68	0.000847	1.35	13.47
4	38.05	154.01	440.55	1.98	726.57	0.001376	1.67	46.72
5	38.00	163.00	505.10	1.98	282.59	0.003539	1.82	67.61
6	2.00	62.69	457.64	1.98	10.09	0.099074	1.84	14.49
7	1.00	450.00	465.44	1.63	0.48	2.075798	7.78	173.49
8	1.00	376.78	386.95	1.63	0.54	1.867499	7.67	128.23
9	1.00	229.01	232.29	1.63	0.69	1.442890	7.40	52.12
10	1.00	150.17	151.58	1.63	0.82	1.217580	7.22	22.22
11	1.00	25.00	104.93	20.34	997.05	0.001003	0.37	0.35
12	2.00	25.01	105.05	20.34	997.09	0.001003	0.37	0.45
13	1.50	30.01	125.91	20.34	995.67	0.001004	0.44	1.06

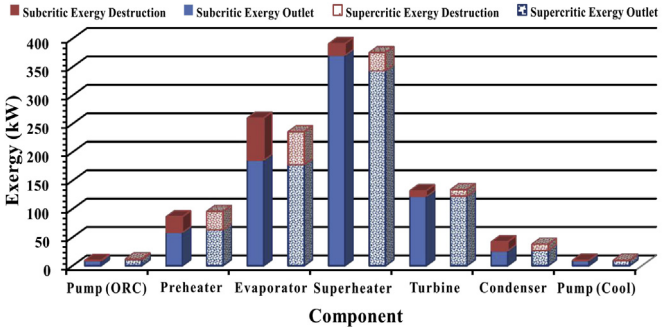


Fig. 9. The exergy exit and destruction rate of the improved subcritical and supercritical ORC.

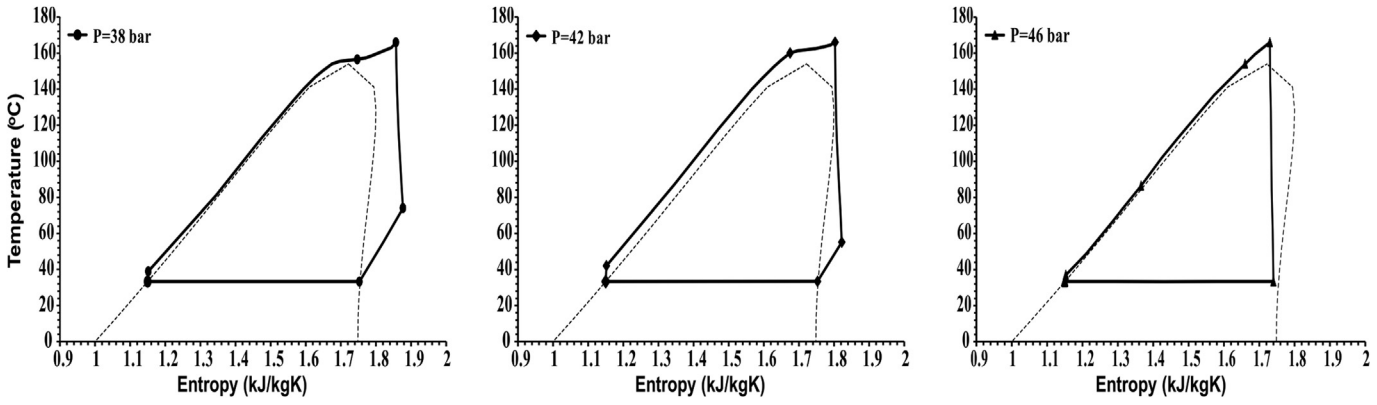


Fig. 8. Temperature and entropy change diagram of the supercritical ORC for 38 bar, 42 bar and 46 bar of turbine inlet pressure at maximum temperature of R245fa (166 °C).

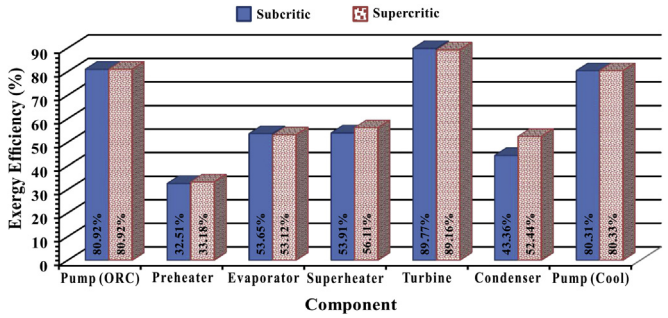


Fig. 10. The exergy efficiency of the improved subcritical and supercritical ORC components.

27.76%, respectively. The increase in efficiency is directly related to the decrease of exergy destruction. It can be seen that total exergy loss of the supercritical condition are lower in general and the minimum of the exergy losses correlates with the maximum of the system exergetic efficiency.

The maximum working temperature of the ORC is limited as 166 °C which is equal to the maximum temperature of the R245fa and the turbine inlet temperature of the best performed subcritical and supercritical ORC is almost equal. The entropy value of the turbine output of subcritical ORC is bigger than supercritical ORC. Therefore, exergy efficiency of the condenser of subcritical ORC is lower than condenser of supercritical ORC, because of more exergy destruction in the condenser of subcritical ORC.

5. Conclusion

In this paper, subcritical and supercritical ORC designed and improved for exhaust waste heat of CHP engine. The positive relation between turbine inlet temperature and pressure was observed with respect to net power, mass flow rate, pumps total power consumption, total evaporator exergy inlet, thermal efficiency and exergy efficiency. Another important parameter affecting the chemical composition of the working fluid and system performance is a maximum temperature of the working fluid.

In the subcritical ORC performance analysis, three different changes in net power, thermal efficiency and exergy efficiency were observed with increasing turbine inlet temperature and constant turbine inlet pressure. The results show almost linear decreasing of net power, thermal efficiency and exergetic efficiency up to 12 bar of turbine inlet pressures, between 12 and 24 bar of turbine inlet pressure there is an increase of the results with rising temperature until a certain point and then values start to decrease. Over the 24 bar of turbine inlet pressure results always increase with increasing temperature at constant turbine inlet pressure level. The variation in the results might cause by the non-linear change of mass flow rate and enthalpy. The best performed supercritical ORC was evaluated at near the maximum temperature of the working fluid, R245fa. Therefore, to protect cycle performance and working fluid composition the turbine inlet temperature of the best performed supercritical ORC was selected as about 1 °C below the maximum temperature. Consequently, the net power, thermal efficiency and exergy efficiency parameters of the subcritical ORC calculated as 79.23 KW, 15.51% and 27.20% at 30 bar 165 °C.

Compared to the subcritical ORC, the supercritical ORC can lead the make better net power, energy efficiency and exergy efficiency. The performance results of the supercritical ORC rise with increasing turbine inlet temperature at constant pressure. The maximum net power, thermal efficiency and exergy efficiency was evaluated as 81.52 kW, 15.93% and 27.76% at 38 bar 163 °C in the case of supercritical ORC, respectively.

Additionally, second law analyses were evaluated and compared for the ideal turbine inlet temperature and pressure of the subcritical and supercritical ORC which occur at 30 bar 165 °C and 38 bar 163 °C, respectively. The maximum exergy destruction of the component was determined in the evaporator for both subcritical and supercritical ORC. The minimum and maximum exergy efficiency of the cycle components was occurred at preheater and turbine, respectively. The overall exergy efficiency of the subcritical and supercritical ORC was calculated as 27.20% and 27.76%, respectively. In spite of the best performance results of the supercritical ORC, detailed thermo-economic analysis and comparison should be made to decide which cycle has ideal repayment period.

Acknowledgements

The authors are grateful for the information and data provided by Tom De Vrieze from Vanheede Environment Group; Bruno Vanslambrouck and Martijn van den Broek from Ghent University; Marc J. M. Van Wonterghem from BEP Europe.

Nomenclature

CHP	combined heat and power
CW	cooling water
$\dot{E}_{ex}$	exergy flow (kW)
h	enthalpy (kJ/kg)
JW	jacket water
$\dot{m}$	mass flow (kg/s)
ORC	organic Rankine cycle
P	pressure (bar)
$\dot{Q}$	heat flow (kW)
s	entropy (kJ/kgK)
T	temperature (°C)
T_0	environment temperature (°C)
$\dot{W}$	power (kW)
v	specific volume (m^3/kg)

Greek letters

ρ	density (kg/m^3)
ψ	specific exergy (kJ/kg)
ε	exergy efficiency (%)
η	energy efficiency (%)

Subscripts

c	condenser
CW	cooling water
des	destruction
e	evaporator
ex	exergy
exh	exhaust
in	inlet
out	outlet
p	pump
ph	preheater
rev	reversible
sh	superheater
t	turbine

References

[1] International Energy Agency. World energy outlook 2012 factsheet [cited 2015 Nov 7]. Available from: httpwww.worldenergyoutlook.orgmediaweowebsite2012factsheets.pdf.
[2] Geels FW. Regime resistance against low-carbon transitions: introducing

politics and power into the multi-level perspective. Theory Cult Soc 2014;31(5):21–40.
[3] Mathiesen BV, Lund H, Connolly D, Wenzel H, Østergaard PA, Möller B, et al. Smart energy systems for coherent 100% renewable energy and transport solutions. Appl Energy 2015;145:139–54.
[4] Clancy JM, Gaffney F, Deane JP, Curtis J, Gallachóir BÓ. Fossil fuel and CO_2 emissions savings on a high renewable electricity system–a single year case study for Ireland. Energy Policy 2015;83:151–64.
[5] Chynoweth DP, Owens JM, Legrand R. Renewable methane from anaerobic digestion of biomass. Renew Energy 2001;22(1):1–8.
[6] Koroneos C, Spachos T, Moussiopoulos N. Exergy analysis of renewable energy sources. Renew Energy 2003;28(2):295–310.
[7] Barbir F. PEM electrolysis for production of hydrogen from renewable energy sources. Sol Energy 2005;78(5):661–9.
[8] Demirbas A. Potential applications of renewable energy sources, biomass combustion problems in boiler power systems and combustion related environmental issues. Prog Energy Combust Sci 2005;31(2):171–92.
[9] Mert I, Karakus C. A statistical analysis of wind speed data using Burr, generalized gamma, and Weibull distributions in Antakya, Turkey. Turkish J Electr Eng Comput Sci 2015;23(6):1571–86.
[10] Bedoya ID, Saxena S, Cadavid FJ, Dibble RW, Wissink M. Experimental evaluation of strategies to increase the operating range of a biogas-fueled HCCI engine for power generation. Appl Energy 2012;97:618–29.
[11] Budzianowski WM. Sustainable biogas energy in Poland: prospects and challenges. Renew Sustain Energy Rev 2012;16(1):342–9.
[12] Tian H, Shu G, Wei H, Liang X, Liu L. Fluids and parameters optimization for the organic Rankine cycles (ORCs) used in exhaust heat recovery of internal combustion engine (ICE). Energy 2012;47(1):125–36.
[13] Abusoglu A, Kanoglu M. Exergetic and thermoeconomic analyses of diesel engine powered cogeneration: part 2–application. Appl Therm Eng 2009;29(2):242–9.
[14] He M, Zhang X, Zeng K, Gao K. A combined thermodynamic cycle used for waste heat recovery of internal combustion engine. Energy 2011;36(12):6821–9.
[15] Schuster A, Karellas S, Kakaras E, Spliethoff H. Energetic and economic investigation of organic Rankine cycle applications. Appl Therm Eng 2009;29(8):1809–17.
[16] Yamamoto T, Furuhata T, Arai N, Mori K. Design and testing of the organic Rankine cycle. Energy 2001;26(3):239–51.
[17] Hettiarachchi HM, Golubovic M, Worek WM, Ikegami Y. Optimum design criteria for an organic Rankine cycle using low-temperature geothermal heat sources. Energy 2007;32(9):1698–706.
[18] Chen Q, Xu J, Chen H. A new design method for organic Rankine cycles with constraint of inlet and outlet heat carrier fluid temperatures coupling with the heat source. Appl Energy 2012;98:562–73.
[19] Lakew AA, Bolland O. Working fluids for low-temperature heat source. Appl Therm Eng 2010;30(10):1262–8.
[20] Tian H, Liu L, Shu G, Wei H, Liang X. Theoretical research on working fluid selection for a high-temperature regenerative transcritical dual-loop engine organic Rankine cycle. Energy Convers Manag 2014;86:764–73.
[21] Al-Sulaiman FA, Dincer I, Hamdullahpur F. Thermoeconomic optimization of three trigeneration systems using organic Rankine cycles: part II–applications. Energy Convers Manag 2013;69:209–16.
[22] Gu Z, Sato H. Optimization of cyclic parameters of a supercritical cycle for geothermal power generation. Energy Convers Manag 2001;42(12):1409–16.
[23] Schuster A, Karellas S, Aumann R. Efficiency optimization potential in supercritical organic Rankine cycles. Energy 2010;35(2):1033–9.
[24] Algieri A, Morrone P. Comparative energetic analysis of high-temperature subcritical and transcritical organic Rankine cycle (ORC). A biomass application in the Sibari district. Appl Therm Eng 2012;36:236–44.
[25] Srinivasan KK, Mago PJ, Krishnan SR. Analysis of exhaust waste heat recovery from a dual fuel low temperature combustion engine using an organic Rankine cycle. Energy 2010;35(6):2387–99.
[26] Qiu G, Shao Y, Li J, Liu H, Riffat SB. Experimental investigation of a biomass-fired ORC-based micro-CHP for domestic applications. Fuel 2012;96:374–82.
[27] Kölsch B, Radulovic J. Utilisation of diesel engine waste heat by organic Rankine cycle. Appl Therm Eng 2015;78:437–48.
[28] Abusoglu A, Kanoglu M. Exergetic and thermoeconomic analyses of diesel engine powered cogeneration: part 1–formulations. Appl Therm Eng 2009;29(2):234–41.
[29] Al-Sulaiman FA, Dincer I, Hamdullahpur F. Exergy analysis of an integrated solid oxide fuel cell and organic Rankine cycle for cooling, heating and power production. J Power Sources 2010;195(8):2346–54.
[30] Cengel YA, Boles MA. Thermodynamics: an engineering approach. 6th Ed. New York: McGraw-Hill Inc.; 2008.
[31] Bejan A, Tsatsaronis G, Moran M. Thermal design and optimization. New York: John Wiley; 1996.
[32] NIST. Reference fluid thermodynamic and transport properties (REFPROP). Version 9.0.
[33] Quoilin S. Experimental study and modeling of a low temperature Rankine cycle for small scale cogeneration. Thesis. University of Liege; 2007.
[34] Shengjun Z, Huaixin W, Tao G. Performance comparison and parametric optimization of subcritical organic rankine cycle (ORC) and transcritical power cycle system for low-temperature geothermal power generation. Appl Energy 2011;88(8):2740–54.
[35] Braimakis K, Preißinger M, Brüggemann D, Karellas S, Panopoulos K. Low grade waste heat recovery with subcritical and supercritical organic Rankine cycle based on natural refrigerants and their binary mixtures. Energy 2015;88:80–92.